Brain, Behavior, & Immunity - Health 2 (2020) 100027

Contents lists available at ScienceDirect

Brain, Behavior, & Immunity - Health

journal homepage: www.editorialmanager.com/bbih/default.aspx

Full Length Article

Retinal-glia ischemia and inflammation induced by chronic stress: The SABPA study

Leoné Malan [a,*], Mark Hamer [b], Roland von Känel [c], Roelof D. van Wyk [d], Annemarie Wentzel [a], Hendrik S. Steyn [e], Pieter van Vuuren [f], Nico T. Malan [a]

[a] Hypertension in Africa Research Team (HART), North-West University, Potchefstroom, 2520, South Africa
[b] Division Surgery & Interventional Science, University College London, United Kingdom
[c] Department of Consultation-Liaison Psychiatry and Psychosomatic Medicine, University Hospital Zurich, 8091, Switzerland
[d] Surgical Ophthalmologist, 85 Peter Mokaba Street, Potchefstroom, 2531, South Africa
[e] Statistical Consultation Services, North-West University, Potchefstroom, 2520, South Africa
[f] School of Electrical, Electronic and Computer Engineering, North-West University, Potchefstroom, 2520, South Africa

ARTICLE INFO

Keywords:
Stress
Ischemia
Inflammation
Retina
Glia

ABSTRACT

Background: Psychobiological processes linking stress and vascular diseases remain poorly understood. The retina and the brain share a common embryonic-diencephalon origin and blood-barrier physiology e.g. ongoing ischemia facilitates S100B release with astrocytic activity and glial-fibrillary-acidic-protein expression (GFAP). However, GFAP decreases revealed astrocyte pathology in the prefrontal cortex of depression/suicide cases; and might be a key mechanism in stress – disease pathways.

Methods: A chronic emotional stress phenotype independent of age, ethnicity or sex was used to stratify the current prospective cohort (N = 359; aged 46 ± 9 years) into Stress (N = 236) and no-Stress groups (N = 123). Prospective data for glia ischemia risk markers were obtained, including 24 h BP, fasting S100B, GFAP, HbA_{1C} and tumor-necrosis-factor-α (TNF-α). At 3-yr follow-up: diastolic-ocular-perfusion-pressure (indicating hypo-perfusion risk) was measured and retinal vessel calibers were quantified from digital images in the mydriatic eye.

Results: Higher hypertension (75% vs. 16%), diabetes (13% vs. 0%) and retinopathy (57% vs. 45%) prevalence was observed in Stress compared to no-Stress individuals. Stressed individuals had consistently raised S100B, TNF-α, HbA_{1C} and higher diastolic-ocular-perfusion-pressure, but decreases in GFAP and GFAP:S100B. Furthermore stroke risk markers, arterial narrowing and venous widening were associated with consistently raised S100B, GFAP:S100B ($p = 0.060$), TNF-α and higher diastolic-ocular-perfusion-pressure [Adj. R^2 0.39–0.41, $p \leq 0.05$]. No retinal-glia associations were evident in the no-Stress group.

Conclusions: Retinal-glia ischemia and inflammation was induced by chronic stress. Persistent higher inflammation and S100B with GFAP decreases further reflected stress-induced astrocyte pathology in the human retina. It is recommended to increase awareness on chronic stress and susceptibility for brain ischemia.

1. Introduction

Emotional stress (coined stress) was associated with sub-clinical neurovascular dysregulation (Lucassen et al., 2014). Stress indeed facilitated astrocytic release of calcium-binding glycoprotein S100B in rodent models inducing ongoing ischemia (Mathea and Newman, 2006). Concomitant activation of the hypothalamic-pituitary-adrenal-axis (HPAA) (Simard et al., 2018; Sild et al., 2017) could therefore link stress and glial damage induced by ischemia.

Astrocytes are the most abundant glia cells in the central nervous system (CNS) and communicate with each other through calcium waves, glial activation, gliotransmitter release and proinflammatory cytokine-induction, e.g. tumor necrosis factor-alpha (TNF-α) (Bender et al., 2016). Glial-fibrillary-acidic-protein expression (GFAP) is an intermediate filament protein and correlate of S100B release (Matias et al., 2019; Yang and Wang, 2015). GFAP reflects astrocyte activation or reactive astrogliosis (Matias et al., 2019) and acts as a calcium sensor (Yang and Wang, 2015). Reactive astrogliosis has been related to concomitant upregulation of GFAP, whereas downregulation was observed in depression/suicide cases, characterized by a decrease in astrocyte density

* Corresponding author. Hypertension in Africa Research Team (HART), North-West University, Private Bag X6001, Potchefstroom, 2520, South Africa.
E-mail address: leone.malan@nwu.ac.za (L. Malan).

https://doi.org/10.1016/j.bbih.2019.100027
Received 28 November 2019; Received in revised form 14 December 2019; Accepted 15 December 2019
Available online 17 December 2019
2666-3546/© 2019 North-West University. Published by Elsevier Inc. This is an open access article under the CC BY-NC-ND license (http://creativecommons.org/licenses/by-nc-nd/4.0/).

in the prefrontal cortex and amygdala (Torres-Plata et al., 2016). Ischemic conditions further altered neuron and glia cell signaling in the retina (Lee and Chung, 2019) and S100B protein was found to be concentrated in astrocytes of retinal neural layers (Kuehn et al., 2018) (Fig. 1). Indeed, S100B and GFAP were notably visible in astrocytes and Müller cells, and more apparent in diabetic patients (Vujosevic et al., 2015).

Both S100B and GFAP may therefore increase risk for neural damage, as S100B-intravitreal injections induced ischemia and glaucoma-like symptoms with early optic nerve axon degeneration followed subsequently by retinal damage (Kuehn et al., 2018; Vujosevic et al., 2015; Hansen et al., 2012). In addition, reduced ocular blood flow to the optic nerve head is facilitated by higher blood pressure and/or lower intra-ocular pressure with increases in vascular resistance and ischemia (Hansen et al., 2012). As diastolic ocular venous pressure is similar or slightly higher than intraocular pressure, it can be estimated as the difference between diastolic blood pressure and intra-ocular pressure, reflecting diastolic-ocular-perfusion-pressure, as a marker of hypo-perfusion (Flammer et al., 2013; Malan et al., 2016a). We therefore aimed to assess ischemia risk in retinal-glia markers [retinal vessel calibers, diastolic-ocular-perfusion-pressure, TNF-α, and glia cell signaling (S100B, GFAP)] in a multi-ethnic cohort.

A hypothesis-driven approach over three decades enabled quantification and validation of a chronic emotional stress phenotype (Filed: Provisional RSA patent application number: 2019/05103). The phenotype revealed good discriminatory ability with a positive prediction of cerebro-cardiovascular disease risk in a prospective cohort, independent of age, ethnicity or sex [Area under the receiver operating characteristic curve: 0.77 ($P \leq 0.001$); 85% sensitivity]. The phenotype was determined with standardized methods (Malan et al., 2015, 2016a, 2017a, 2017b) and applied for the first time to expand knowledge on brain, behavior and immunity function in humans.

2. Materials and methods

2.1. Design and participants

A teachers' cohort (20–65 years) from the Sympathetic activity and Ambulatory Blood Pressure in Africans (SABPA) prospective study was followed for 3 years (Fig. 2), and the study is well-described elsewhere (Malan et al., 2015). The rationale for the selection of the participants was to obtain a sample from a homogenous working environment with similar socio-economic status. Seasonal changes were avoided and extensive clinical assessments were to be performed in a well-controlled temperature and light setting. Exclusion criteria were pregnancy, lactation, tympanum temperature above 37.5 °C, the use of psychotropic substances or α- and β-blockers and blood donors or individuals vaccinated within 3 months prior to data collection.

Only teachers participating in both phases (N = 359) were included for the current investigation. Participants were fully informed about the objectives and procedures prior to recruitment and provided written, informed consent. The study conformed to the Helsinki Declaration (2004) and was approved by The Ethics Review Board of the North-West University, South Africa: Approval number NWU-0003607S6.

2.2. Cardiovascular measurements

A combined ambulatory blood pressure-electrocardiogram apparatus (Cardiotens CE120®, Meditech, Budapest Hungary) was applied between 07:00–09:00 on working days (Monday-Thursday) at the teachers' school

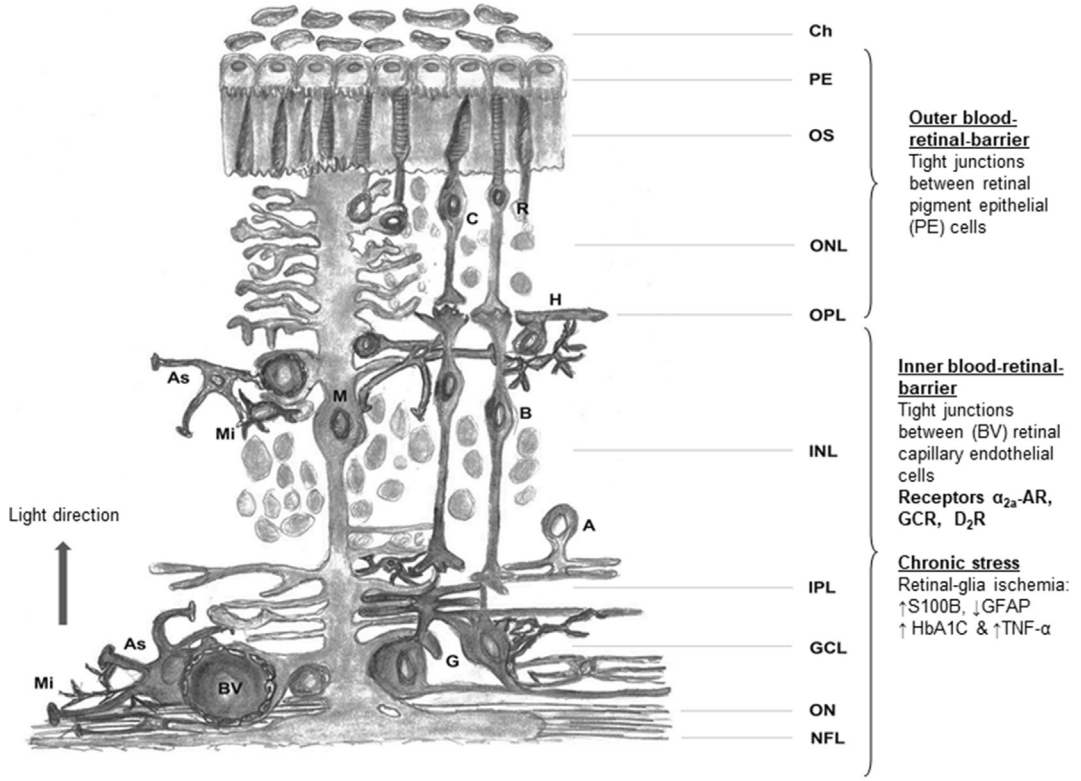

Fig. 1. Representation of retinal-glia vascular communication in the human adult retina. Light direction is from the bottom to the top. The *inner blood retinal barrier* contains: NFL, optic nerve fiber layer; ON, optic nerve; GCL, ganglion cell layer; IPL, inner plexiform layer; INL, inner nuclear layer; OPL, outer plexiform layer with Horizontal cells (H), Bipolar cell dendrites (B), Microglia (Mi); Astrocytes (As); Amacrine cells (A), Müller cells (M). Stress hormones receptors (alpha$_{2a}$-adrenergic, α_{2a}-AR), glucocorticoid (GCR) and dopamine$_2$ (D_2R) are expressed in Müller and Amacrine cells. S100B and glial-fibrillary-acidic-protein (GFAP) are expressed in Astrocytes and Müller cells. The *outer blood retinal barrier* contains: ONL, outer nuclear layer with rods (R) and cones (C); OS; outer segment layers; PE, pigment epithelium; Ch, choroid (*Drawn by Louise Malan).*

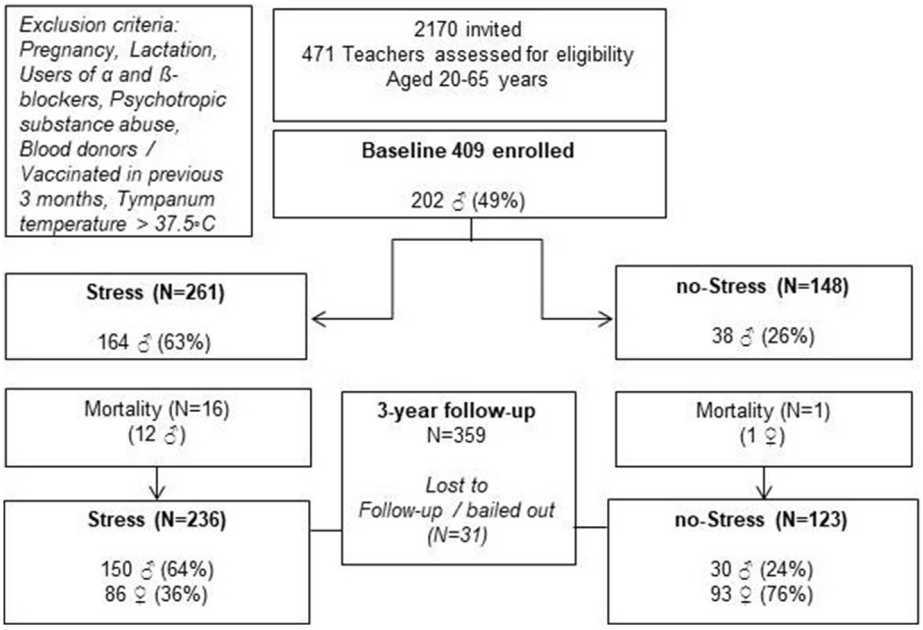

Fig. 2. The Sympathetic activity and Ambulatory Blood Pressure in African (SABPA) prospective cohort stratified into Stress and no-Stress phenotype groups.

of employment. The blood pressure cuff was fitted to the non-dominant arms using an appropriate cuff size. Blood pressure measures were obtained every 30 min during the day (08:00–22:00) and hourly during the night (22:00–06:00). Participants continued their usual daily activities and were asked to record occurrences of stress, physical activity, headache, syncope, dizziness, nausea, palpitations, hot flushes and visual disturbances on their ambulatory diary card. The 24 h successful inflation rate was 77.9% (±12.9) in Stressed individuals and 81.8% (±10.1) in no-Stressed individuals. The data were analyzed with the CardioVisions 1.19 Personal Edition software (Meditech, Budapest, Hungary). Hypertensive status was classified as 24 h SBP ≥130 mm Hg and/or DBP ≥80 mm Hg (Piepoli et al., 2016).Participants resumed their normal school and extra-curricular activities till 15:00 and hereafter transported to the North-West University for clinical measures including retinal vessel imaging and depression status evaluation under supervision of clinical psychologists. They fasted from 22:00 till 07:00 when anthropometric measures as well as blood samples were collected followed by carotid intima media screening and physical activity measures.

2.3. Retinal vessel analyses (RVA)

Participants abstained from food or caffeine containing beverages, alcohol, smoking or exercise 1 h prior to measurements. Participants were introduced to the procedure by a trained registered nurse and screened for acute anterior angle chamber glaucoma risk with a small light source. Mydriasis was induced in the right eye of the participant by means of a drop containing tropicamide, 1% and benzalkonium chloride 0.01% (m/v). Fundus imaging was performed in a well-controlled light and temperature regulated room with the retinal vessel analyzer with a Zeiss FF450^{Plus} camera and the software VesselMap 2, Version 3.02 (Imedos Systems GmbH, Jena, Germany). Retinal vessel calibers were measured as monochrome images by manually selecting first order vessel branches in a measuring zone located between 0.5 and 1.0 optic disc diameters from the margin or the optic disc. Upon selection of the vessel, software automatically delineated the vessels' measuring area. A color image was used as reference to ascertain correct identification of arteries and veins and two experienced scientists agreed on the vessel type before selection. Automated software calculations, based on the Knudtson formula, determined estimates from the 6 largest arteries and veins. As the image scale of each eye was unknown, the values of the retinal arteries and veins were expressed as measuring units (MU). 1 MU is equivalent to 1 μm when the dimensions of the eye being examined correspond to those of the normal Gullstrand eye. Reproducibility was computed for a randomly selected cohort with a correlation coefficient of 0.84.

2.4. Diastolic ocular perfusion pressure (hypo-perfusion risk)

A local anesthetic drop (Novasine Wander 0.4% Novartis) was inserted in the right eyes in 99% of all cases to measure intra-ocular pressure (IOP) with the Tono-Pen Avia Applanation Tonometer (Reichert 7–0908, ISO 9001, New York, USA). Right eye diastolic-ocular perfusion-pressure (mmHg) was calculated (DBP minus intra-ocular pressure) and hypertensive/diabetic retinopathy was diagnosed by a registered ophthalmologist.

2.5. Depression

The severity of depressive symptoms was assessed with the Patient Health Questionnaire (PHQ-9), which contains 9 items and has been validated in various ethnic groups for use in primary health care settings (Kroenke and Spitzer, 2002). Each item evaluates the presence of one of the nine Diagnostic and Statistical Manual of Mental Disorder Fourth Edition (DSM-IV) criteria for depression. The Cronbach's alpha-reliability index for the total PHQ-9 score in the current cohort was 0.80 indicating good reliability. Moderate-to-severe depressed (PHQ-9 score ≥ 10) and severe depressed cases (PHQ-9 score ≥15) are clinically relevant.

2.6. Anthropometric measures

Registered level II anthropometrists measured waist circumference to indicate central obesity (Hoebel et al., 2014) in triplicate with a non-extensible and flexible anthropometric tape with intra- and inter variability less than 5%. Total energy expenditure (kCal) over 7 days was derived from the Actiheart accelerometer (GB06/67703; CamNtech Ltd, Upper Pendrill Court, Papworth Everard, Cambridgeshire, CB233UY, UK).

2.7. Carotid intima media thickness

High resolution ultrasound images were acquired from at least two

optimum angles of the common carotid artery segments [Sonosite Micromaxx ultrasound system (SonoSite Inc., Bothell, WA, USA) and 6–13 MHz linear array transducer] using the Rudy Meijer protocol. The images were digitized and imported into the Artery Measurement Systems automated software (AMS) II v1.139 (Gothenburg, Sweden) for dedicated analysis of the carotid artery as ischemic stroke risk marker (Piepoli et al., 2016). For the purpose of this study, the left far wall measurements were used to estimate left far wall carotid intima media thickness (L-CIMTf). Carotid bifurcation stenosis was determined at follow-up by a registered sonar technologist and added as covariate in retinal models. Intra-observer variability was 0.04 mm between two measurements made 4 weeks apart on 10 participants.

2.8. Biochemical analyses

Participants were in a semi-recumbent position for at least 30 min before 09:00 in both study phases. A registered nurse obtained fasting blood samples from the antebrachial vein branches of the dominant arm of each participant with a winged infusion set and she also performed pre- and post-counselling for HIV positive status participants. All blood samples were handled according to standardized procedures and stored at −80 °C until analyses. All biochemical analyses were done in duplicate on never thawed serum/plasma samples. Serum lipids were analyzed with an enzyme rated method (Unicel DXC 800 - Beckman and Coulter, Germany). Serum gamma glutamyl transferase (GGT) and whole blood EDTA glycated hemoglobin (HbA_{1C}) were analyzed with turbidimetric inhibition immunoassays (Cobas Integra 400 Plus, ROCHE Basel, Switzerland). The American Diabetes Foundation guidelines were used to define diabetic status ($HbA_{1C} \geq 6.5\%$). HIV positive status was determined with a rapid antibody test in plasma (First response kit. PMC Medical, Daman, India) and confirmed with the Pareekshak test (BHAT Bio-Tech, Bangalore, India). Serum S100B was analyzed with an electrochemiluminescence immunoassay (e411, ROCHE, Basel, Switzerland) with intra- and inter-assay coefficients of less than 5%.

DuoSet ELISA kits (Catalogue #DY2594-05) from R&D Systems Inc. (Minneapolis, USA) were used for serum Human GFAP analyses with low intra- (3.96%) and inter-assay (1.63%) variation. Serum cotinine and TNF-α were analyzed at an accredited pathology laboratory (AMPATH, Gauteng, South Africa). Serum cotinine values were derived from a homogeneous immunoassay (Modular ROCHE Automized systems, Basel, Switzerland) and serum TNF-α values from a quantikine high sensitivity human TNF-α enzyme-linked immunosorbent assay (HS ELISA; R&D Systems, Minneapolis, MN USA). The inter- and intra-assay variability for TNF-α was 15% and 17.8%, respectively.

2.9. Statistical analyses

Statistica version 13.3 (TIBCO Software Inc., Palo Alto, USA, 2018) was used for data analyses. A chronic emotional stress phenotype was used to stratify the cohort into Stress (n = 236) and no-Stress (n = 123) groups. Normal distribution was computed and skewed data were log-transformed. Independent T tests compared Stress vs. no-Stress groups whilst proportions and prevalence were determined by using chi-square (χ^2) statistics. Effect sizes when comparing means are reported as *d*-values with 0.2 = small effect, 0.5 = medium effect and 0.8 = large effect. When reporting beta-coefficients or OR as an effect size, the following guideline values were used: 1.5 = small effect, 2.5 = medium effect and 4.25 = large effect. Mean changes over 3yrs of each variable within Stress and no-Stress groups and also in 10 deceased cases were calculated using dependent sample t-tests. McNemar's case-control tests were computed to determine incidence and recovery frequencies over 3 yrs. Retinal vessel calibers and diastolic-ocular-perfusion-pressure differences were compared between Stressed vs. no-Stressed groups using single one-way ANCOVA's, considering age and the vessel type.

Multiple linear regression analyses determined associations between retinal vessel diameters, glia and perfusion risk markers in the Stress and no-Stress groups. Baseline *a-priori* selected covariates were age, waist circumference, cotinine, GGT, HbA_{1c}, total chol:HDL, TNF-α, as well as carotid bifurcation stenosis, hypertensive/diabetic retinopathy and diastolic-ocular-perfusion-pressure obtained at follow-up. When the retinal artery was a dependent variable, the retinal venous diameter was included as covariate and vice versa. Dependent variables included retinal artery and -venous vessel calibers. Independent covariates included *a-priori* selected covariates delineated above and glia cell risk markers in separate models. Model 1: included baseline S100B and/or GFAP or GFAP:S100B; Model 2 included follow-up S100B and/or GFAP or GFAP:S100B; and Model 3 included 3-yr changes in S100B and/or GFAP or GFAP:S100B. Three year percentage changes (Δ) were calculated as follows: 3yr follow-up – baseline/baseline x 100.

In sensitivity analyses:

a) Regression analyses were repeated to consider HIV positive status; as well as moderately severe depression (PHQ-9 score >10).
b) We stratified the chronic emotional stress phenotype into three equally sized groups after ordering the values from smallest to largest in order to more finely differentiate the stressed participants (no Stress; mildly Stressed and very Stressed). Statistical analyses were repeated to detect changes in glial and retinopathy risk markers over 3 years using dependent samples T tests. Linear regression analyses followed to assess associations between retinal vessel changes and risk markers in the three groups. The dependent variables included retinal artery and -venous vessel calibers; and the independent covariates included *a-priori* selected covariates.

The statistical significance level was set at $p \leq 0.05$ (two-tailed). The F to enter in regression models was fixed at 2.5.

3. Results

A total of 359 participants with a mean age of 45.6 ± 9.1 years were followed for 3 years. In Table 1, more men (64%) were classified of having chronic stress compared to their female counterparts (36%).

A higher mortality count was observed in Stress individuals (n = 16; 53 ± 7.3 years) vs. the no-Stress individual who passed away after a vehicle head on collision (n = 1) (p = 0.02). The higher mortality count in Stress individuals was caused by various diseases: stroke (N = 2), kidney/heart failure (N = 3), cancer (N = 2), diabetes (N = 4), coronary disease/event (N = 4), and suicide (N = 1). Stress individuals had more cardiometabolic perturbations with medium - high effect sizes ($p \leq 0.001$) with higher central obesity (d = 0.5, medium effect), total cholesterol:HDL > 5 and HbA_{1C} (d ≥ 0.8, large effect); TNF-α (d = 0.4, moderate effect) and 24 h blood pressure (d = 1, large effect) than non-Stress individuals. Glial cell risk markers were similar with small effect sizes in the Stress vs. no-Stress groups, S100B (d = 0.32), GFAP (d = 0.13) and GFAP:S100B (d = 0.12). The Stress vs. no-Stress group showed higher diastolic-ocular-perfusion-pressure (d = 0.8, large effect) and narrower arteries (d = 0.5, medium effect); higher prevalence for 24 h hypertension (75% vs. 16%); diabetes (13% vs. 0%), hypertensive/diabetic retinopathy (57% vs. 47%), arteriovenous nicking (48% vs. 32%), and usage of more ACE inhibitors (10% vs. 2%), calcium channel blockers (6% vs. 0%) and thiazides (13% vs. 1%).

Three year changes in glia cell risk markers with respect to the stress phenotype are shown in Fig. 3.

A similar profile was observed in the Stress death/mortality cases (Fig. 3a) as in the total Stress cohort (Fig. 3b), namely consistently raised S100B, TNF-α and HbA_{1C} levels with decreases in GFAP. In Table S1, consistently raised GGT, SBP and decreases in the GFAP:S100B ratio in Stressed individuals and in mortality cases were observed. Low incidence frequencies for hypertension (5%) and diabetes (3%) were apparent with greater recovery frequencies in hypertension (16%), and almost absent in

Table 1
Comparing the clinical characteristics of the chronic emotional stress phenotype cohort (Stress vs. no-Stress).

	Stress (n = 236)	no-Stress (n = 123)	P-values	d-values
Age (years)	46.3 (8.9)	44.3 (9.0)	0.047	0.22
Black/Whites, n (%)	129/107 (55/45)	44/79 (36/64)		
Men, n (%)	150 (64)	30 (24)	<0.001	0.78
Physical activity (kCal/7 days)	3394.1 (1513.1)	3199.5 (1099.0)	0.210	0.14
Retinal-glia risk markers				
Cotinine (ng/ml)	0.01 (0.01, 0.01)	0.01 (0.01, 0.01)	0.128	0.17
Gamma glutamyl transferase (U/l)	33.6 (21.0, 61.4)	20.0 (12.0, 37.8)	<0.001	0.32
Waist circumference (cm)	98.2 (88.7, 106.3)	83.3 (74.6, 93.4)	<0.001	0.89
Total cholesterol:HDL	5.2 (2.0)	3.9 (1.1)	<0.001	0.75
HbA_{1c} (%)	6.0 (1.1)	5.5 (0.3)	<0.001	1.35
Tumor necrosis factor-α (pg/ml)	2.5 (1.1, 4.2)	1.4 (0.1, 2.8)	0.047	0.41
24 h SBP (mmHg)	134 (15)	118 (8)	<0.001	1.07
24 h DBP (mmHg)	84 (10)	73 (6)	<0.001	1.10
Intra-ocular pressure (mmHg)	16 (4)	15 (4)	0.044	0.26
Diastolic-ocular-perfusion-pressure (mmHg)	73 (12)	64 (10)	<0.001	0.78
S100B (μg/L)	0.05 (0.0)	0.04 (0.0)	0.421	0.33
S100B (μg/L)	*0.04 (0.03, 0.06)*	*0.04 (0.03, 0.05)*		
GFAP (ng/ml)	29.1 (52.3)	36.5 (61.0)	0.232	0.13
GFAP (ng/ml)	*1.39 (0.2, 31.7)*	*2.28 (0.2, 48.7)*		
GFAP:S100B	815.92 (1580.5)	1013.30 (1741.0)	0.281	0.12
GFAP:S100B	*25.3 (4.5, 938.8)*	*57.2 (5.0, 1397.0)*		
Retinal arterial caliber (MU)	148.5 (11.1)	154.1 (13.4)	<0.001	0.46
Retinal venous caliber (MU)	243.2 (20.0)	240.6 (20.2)	0.267	0.13
Retinopathy, n (%)	134 (57)	55 (45)	0.024	0.24
Retinal arteriovenous nicking, n (%)	110 (48)	38 (32)	0.004	0.32
Optic nerve head damage	21 (9)	8 (7)	0.430	0.09
Moderate-to-severe depression (PHQ-9 ≥ 10), n (%)	69 (29)	40 (33)	0.521	−0.07
Severe depression (PHQ-9 ≥ 15), n (%)	26 (11)	15 (12)	0.739	−0.04
Left-CIMTf ≥ 0.75 mm, n (%)	79 (34)	18 (15)	<0.001	0.42
24 h Hypertension, n (%)	176 (75)	19 (16)	<0.001	1.19
Diabetes	30 (13)	0 (0)	<0.001	0.46
Medications				
Anti-depressants	2 (1)	2 (2)	0.505	−0.07
ACE-inhibitors	23 (10)	2 (2)	0.004	0.32
Aspirin	13 (6)	3 (2)	0.181	0.15
Beta-blockers	6 (3)	1 (1)	0.261	0.13
Calcium channel blockers	14 (6)	0 (0)	0.006	0.31
Diuretics	31 (13)	1 (1)	0.001	0.43
Statins	8 (3)	3 (2)	0.620	0.06

Values are presented as mean (±SD) and/or median (± 95% interquartile range). Abbreviations: HbA_{1C}, glycated hemoglobin; GFAP, glial-fibrillary-acidic-protein; Moderate-severe depression, Patient Health Questionnaire-9/PHQ-9 and Severe depression, PHQ-9≥15 (Kroenke and Spitzer, 2002); Optic nerve head damage, cup-to-disc ratio ≥ 0.3 plus intra-ocular pressure ≥21 mmHg; 24h Hypertension, SBP ≥ 130 and/or DBP ≥ 80 mmHg and L-CIMTf, left-carotid intima media thickness far wall ≥ 0.75 mm (Piepoli et al., 2016); Diabetes (HbA_{1C}, glycated hemoglobin ≥ 6.5 %, American Diabetes Association). Cohen's *d*-values reflected as: 0.2 = small effect, 0.5 = medium effect and 0.8 =large effect.

diabetes (1%). In the non-Stressed individuals, metabolic factors TNF-α, GGT and HbA_{1C} increased over 3-yrs ($p < 0.05$); with no 3yr frequency variance in either hypertensive or diabetic status.

In Fig. 4, retinal calibers and diastolic-ocular-perfusion-pressure are presented adjusting for age and artery/venous vessel diameter. Arterial narrowing, venous widening and diastolic-ocular-perfusion-pressure levels were significantly higher ($p \leq 0.001$) in the Stress vs. the non-Stress group.

Unadjusted regression analyses showed associations between mortality (N = 10), consistent S100B ($r = 0.11$; $p = 0.042$) and down-regulation in GFAP ($r = -0.152$; $p = 0.004$) (*data not shown*). Linear regression associations in the Stress group (Table 2) emerged between retinal artery narrowing, higher diastolic-ocular-perfusion-pressure, consistent S100B and GGT [Adj. R^2 0.39, $p \leq 0.05$]; with small-medium effect.

Venous widening was associated with higher diastolic-ocular-perfusion-pressure, consistent S100B ($p \leq 0.001$), ΔGFAP:S100B decreases ($p = 0.060$); persistent GGT and TNF-α levels [Adj. R^2 0.35–0.41, $p \leq 0.05$]; with small-medium effect. Retinal-glia associations did not change when considering HIV positive status; or when repeating the analyses in moderately-severe depressed cases (PHQ-9 ≥ 10; N = 69). No retinal-glia associations were evident in non-Stressed individuals.

Furthermore, changes over 3-yrs in glial and retinopathy risk markers and mortality rates increased linearly across the mildly and very Stressed groups (Table S2); with the highest risks consistently observed in the Stress phenotype group. Similarly, associations between artery narrowing and venous widening (Table S3) in the mildly and very Stressed groups corroborated findings shown for the Stress phenotype group.

4. Discussion

A chronic stress phenotype independent of age, ethnicity or sex reflected ongoing retinal-glia ischemia with consistently raised hypertension, S100B-immune responsivity and decreases in GFAP, retinal arterial narrowing and -venous widening. All retinal-glia cell associations showed small-to-moderate effects, suggesting clinical relevance for ischemic stroke risk.

Interestingly, retinal-glia ischemia afflicted more men (64%) whilst women appeared to be more resilient (no-Stress group, 72%). Contradictory findings from Stegenga et al. (2012) rather suggested a higher physiological vulnerability in depressed women than in their male counterparts. Whether depression affects men and women similarly is disputable as depressed patients, independent of sex, had diminished gray matter volumes and reduced astrocyte densities in the hippocampus and prefrontal cortex (Krishnan and Nestler, 2008). Contrastingly previous findings (Du and Pang, 2015) did not show any relationship

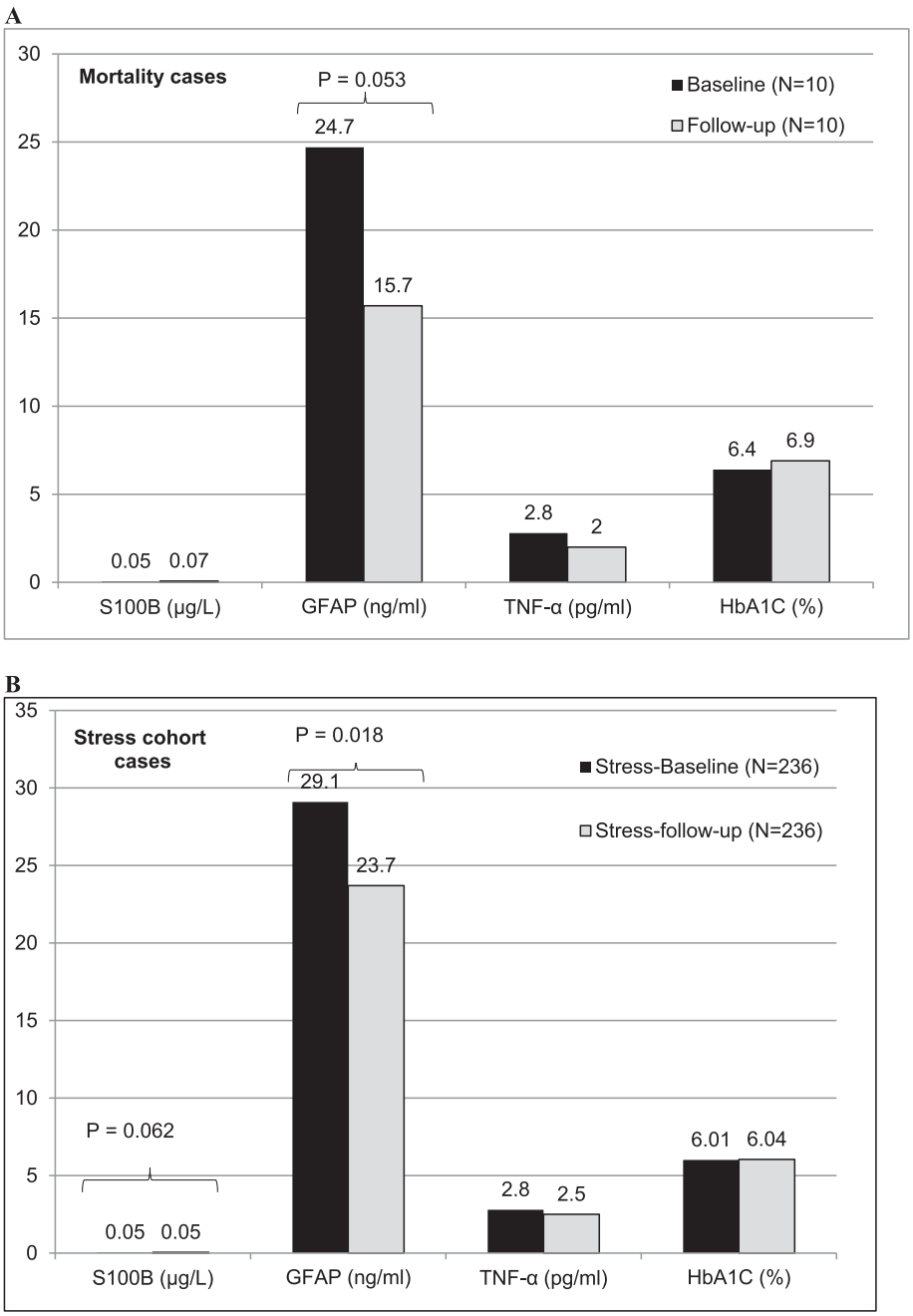

Fig. 3. Presenting changes in retinal-glia risk markers over a period of 3-years in deceased cases from the Stress group (Fig. 3a); and in the total stress cohort (Fig. 3b). Individuals participated at both phases.

between depression and cerebrovascular risk markers. Currently only the Stress phenotype reflected consistently raised S100B and decreased GFAP as markers of stress-related ongoing ischemia. The stress phenotype (quantitative markers) appears to be superior to a qualitative score for depression (e.g. PHQ-9); as moderately-depressed (PHQ-9 $\geq$ 10) cases did not reveal retinal-glia ischemia risk.

4.1. Chronic stress; glia ischemia and inflammatory responsiveness

Glia-ischemia (Wheelock et al., 2016) in the Stress group was reflected by chronically raised S100B and downregulation of GFAP with persistently raised inflammatory markers (TNF-α). Decreases in brain GFAP might be a consequence of astrocyte pathology in limbic cortex areas in depressed/suicide cases (Sild et al., 2017). In rodent models, hippocampal (ventral subiculum) lesions during prolonged stress were accompanied by diminished glucocorticoid-immunoreactivity responsivity (Jauregui-Huerta et al., 2010). Chronic stress may not actually reduce astrocyte numbers but instead could selectively decrease GFAP (Tynan et al., 2013). Stress-induced astrocyte-mediated disturbances may not be due to a loss of cells but rather a consequence of potential changes in synaptic function or even altered receptor function. These changes can indeed facilitate astrocyte and particularly microglia release of gliotransmitters, such as cytokine TNF-α (Stellwagen and Malenka, 2006) as observed in the Stress group; and which may disturb neurovascular communication in the inner blood-retinal-barrier. Serum TNF-α may translate to brain TNF-α as peripheral TNF-α regulated immune cell trafficking in the mouse brain (Paouri et al., 2017), which support our findings of retinal vein widening and associated serum TNF-α responses, reflecting endothelial dysfunction (Liew and Wang, 2011). Venous widening in the Stress group, was related to inflammatory responsivity

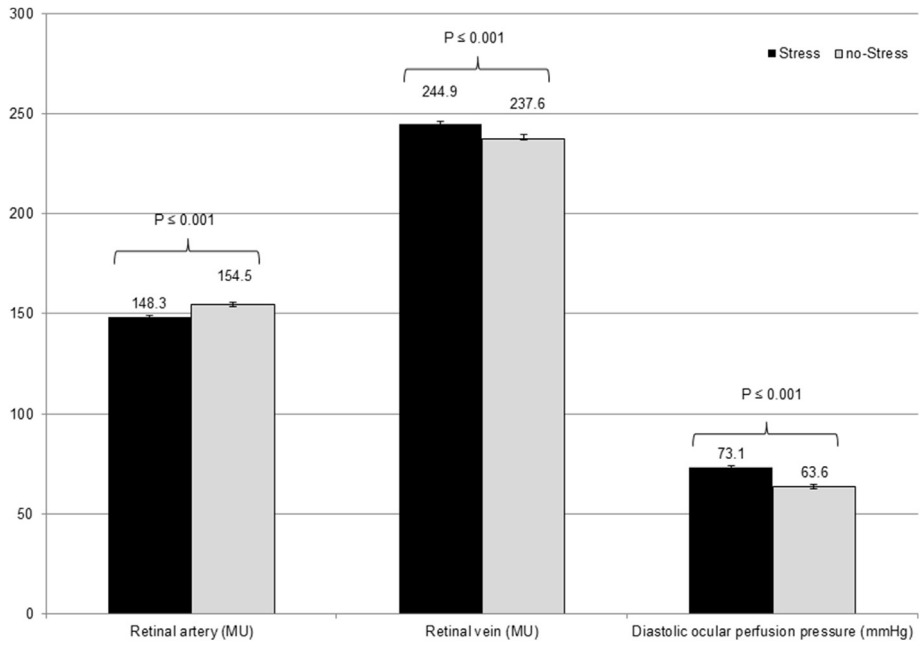

Fig. 4. Comparing (mean ± SE) retinal vessel caliber diameters and diastolic-ocular-perfusion-pressure independent of age in Stressed vs no-Stressed individuals. When the retinal artery was a dependent variable, the retinal vein was included as covariate and vice versa.

and GFAP:S100B decreases, suggestive of GFAP decreases which can reduce activity of GFAP-positive astrocytes (Someya et al., 2019). The stress-induced ongoing ischemia or persistent S100B release will impair myogenic control and increase vascular resistance and -tone (arterial narrowing) (Liew and Wang, 2011; Someya et al., 2019) with potential damage to the retinal ganglion cells and optic nerve head.

Indeed, the similar nature of glia cell signaling in the retina and brain suggests similar neuron and glia-blood vessel or neurovascular communication (Someya et al., 2019; Wentzel et al., 2019). Ischemic stroke risk increases as both carotid intima media thickening and retinal arterial occlusion risk is apparent (Piepoli et al., 2016; Someya et al., 2019; Wentzel et al., 2019; Wu et al., 2017; Malan et al., 2016b) in the Stress group (retinal artery narrowing, venous widening and arteriovenous nicking).

A profile of disturbed neurovascular communication is emerging in the Stress group with ongoing glia ischemia and a composite profile of ocular perfusion deficits, persistent inflammatory responsivity and alcohol abuse or higher GGT levels. Even though GGT levels have also been linked to oxidative stress status and fatty liver disease, higher GGT is a key mechanism by which excessive ethanol consumption promotes tissue injury and inflammatory responsiveness in the brain (Enhörning and Malan, 2019). Zong et al. (2010) indeed suggested that S100B release and GFAP expression, contributed to inflammation-linked responses in retinal neurons. Consistent inflammatory responsivity in the Stress group supports the notion of heightened immune function during chronic emotional “uncontrollable” stress (Wetherell et al., 2017) and hypo-activity in the HPAA (Du and Pang, 2015). Inflammatory responsivity and associated hypertension (Piepoli et al., 2016) with higher diastolic-ocular-perfusion-pressure in stressed individuals could therefore reflect a maladaptive mechanism to compensate for reduced blood perfusion (hypo-perfusion) in the inner blood-retina-barrier.

4.2. Chronis stress, ischemia and hyperglycemia

Susceptibility for artery occlusion and ischemic stroke risk further seems to increase in the Stress group; considering hypo-perfusion and chronic hyperglycemia, which may increase brain insulin-signaling dysfunction and risk for diabetic retinopathy (Díaz-Coránguez et al., 2017). Brain-endothelium insulin receptors may dysregulate kinetics in insulin delivery and neural tissues (Barber et al., 2000). Moreover artery narrowing, venous widening and higher prevalence of arteriovenous nicking in the Stress group suggest diminished vascular tone as glia cell-mediated vasodilation may be reduced (Mathea and Newman, 2006; Kotliar et al., 2017).A prolonged retrograde propagation of the vascular response has indeed been associated with endothelial dysfunction and retinal venous widening (Ito et al., 2003). Chronic hyperglycemia in the Stressed group may partially explain altered metabolic capacity and a reduced ability to maintain blood-retinal-barrier homeostasis in endothelial cells (Dada, 2017) with decreases or downregulation of astrocyte GFAP expression.

The ongoing ischemia in the Stress group reflected consistently raised S100B levels, which increases metabolic demands and higher blood flow or hyperemia (cerebral and retina) to maintain perfusion pressure (Chen and Swanson, 2003). Hyperemia may act as a short-term protective mechanism against pathological conditions. Chronic hyperemia may however be detrimental as the increases in blood flow far exceed the increasing metabolic demand of glia cells and neurons (Mathea and Newman, 2006; Ding et al., 2013) potentially increasing inflammation-driven endothelial dysfunction in the inner blood-retinal-barrier. Future risk for artery occlusion and ischemic stroke may therefore activate downstream signaling pathways and increase the risk for stress-related vascular and neurodegenerative diseases.

4.3. Potential mechanism for retinal-glia ischemia and stroke risk

The findings of our study suggest a potential pathway where chronic stress facilitates ongoing ischemia with astrocyte S100B release and consistent higher or upregulated TNF-α released by microglia. This may occur via engagement of the immune-globulin transmembrane protein receptor for advanced-glycation-end-products (RAGE) (Díaz-Coránguez et al., 2017). Ongoing ischemia and RAGE-mediated transcytosis exemplify endothelial dysfunction (venous widening) and chronic hyperglycemia in the Stress group. A compensatory mechanism or high pressure system can be directly detected by astrocytes, microglia or Müller cells via reactive astrogliosis in an attempt to restore homeostasis in the inner blood-retinal-barrier. Monoamine depletion due to stress may further trigger RAGE activity (Ding et al., 2013) thereby inducing astrocyte calcium waves and altering astrocyte function. Stress-hormone receptors

Table 2
Forward stepwise linear regression analyses depicting associations between retinal vessel calibers and glial cell risk markers in Stressed individuals.

	Stress group (N = 195)	
	Retinal arteries (MU)	Retinal veins (MU)
Model 1: Adjusted R^2	**0.39**	**0.39**
	ß (95% CI), p	*ß (95% CI),p*
DOPP (mmHg)	−0.33 (−0.6, −0.2), p ≤ 0.001	0.23 (0.1, 0.4), p ≤ 0.001
Baseline S100B (μg/L)	−0.12 (−0.3, 0.02), p ≤ 0.050	0.21 (0.1, 0.3), p ≤ 0.001
GGT (U/L)	−0.17 (−0.3, −0.02), p = 0.021	0.14 (0.0, 0.3), p = 0.022
TNF-α (pg/ml)	−0.10 (−0.22, 0.02), p = 0.111	0.13 (0.0, 0.3), p = 0.032
Model 2: Adjusted R^2	**0.38**	**0.41**
	ß (95% CI), p	*ß (95% CI),p*
DOPP (mmHg)	−0.33 (−0.45, −0.21), p ≤ 0.001	0.23 (0.11, 0.35), p ≤ 0.001
Follow-up S100B (μg/L)		0.25 (0.13, 0.37), p ≤ 0.001
GGT (U/L)	−0.20 (−0.32, −0.08), p ≤ 0.001	0.15 (0.03, 0.27), p = 0.017
TNF-α (pg/ml)	–	0.11 (−0.01, 0.23), p = 0.064
Model 3: Adjusted R^2	***<0.10***	**0.36**
	ß (95% CI), p	*ß (95% CI), p*
DOPP (mmHg)		0.25 (0.1, 0.4), p ≤ 0.001
ΔGFAP:S100B (μg/L)		−0.12 (−0.2, 0.0), p = 0.060
GGT (U/L)		0.13 (0.01, 0.3), p = 0.045
HbA_{1C} (%)		0.13 (0.01, 0.3), p = 0.041
TNF-α (pg/ml)		0.12 (0.0, 0.2), p = 0.047

Case-wise deletion was applied with F to enter = 2.5. Additional covariates included cotinine, glycated hemoglobin, total chol:HDL; hypertensive/diabetic retinopathy and carotid bifurcation stenosis. When the retinal artery was a dependent variable, the retinal vein was included as covariate and vice versa. Abbreviations: DOPP, diastolic-ocular-perfusion-pressure; GGT, gamma glutamyl transferase; TNF-α, tumour necrosis factor-α; GFAP, glial fibrillary acidic protein; HbA_{1C}, glycated hemoglobin.

(e.g. glucocorticoid and norepinephrine) are located on the surface of astrocytes (Ding et al., 2013; Chandley et al., 2012); and dysfunctional stress-hormone levels were indeed associated with retinal vascular dysregulation in the SABPA cohort, independent of ethnicity and sex [under review].

The current study is limited by its sample size as larger cohorts are needed to more representatively verify ongoing retinal-glia ischemia. In addition, a more comprehensive profile of glia cell markers should be assessed to provide evidence for stress-related glia pathology in the inner-blood-retinal barrier. Associations between mortality risk, increasing S100B and GFAP downregulation should be further investigated and validated. Strengths of the study include the application of a novel quantified chronic emotional stress phenotype to assess progression of retinal-glia ischemia using gold standard measures and a well-controlled protocol.

In conclusion, chronic stress reflected retinal-glia ischemia and stroke risk. Persistent higher S100B but GFAP decreases related to findings of stress-induced astrocyte pathology in the human retina.

4.4. Translational clinical value

Stress may play an important role in the pathogenesis of synaptic plasticity as ischemic conditions alter neurotrophic signaling, synaptic plasticity and pathophysiology. **A validated Stress phenotype was applied and enabled detection of ischemic stroke susceptibility in the brain-retina axis.** Preventive screening for Stress is recommended as it may improve individual awareness on stress-related ischemic stroke risk.

Author contributions

LM, MH, RvK, NTM, HSS, PvV: conception and design of the study; LM, NTM, AW: acquisition and analysis of data; LM, MH, RvK, RvW, NTM, AW, HSS, PvV: drafting, editing and approval of the final draft.

Declaration of competing interest

None declared.

Acknowledgements

We gratefully acknowledge the voluntary collaboration of the participants. The SABPA study would not have been possible without the valuable contributions from co-investigators and technical staff. Funding sources included the North-West University and North-West Education Department South Africa; Medical Research Council and National Research Foundation South Africa; ROCHE Diagnostics South Africa; Heart and Stroke Foundation South Africa (HSFSA2019/1); and the Metabolic Syndrome Institute, France. Any opinion, findings and conclusions or recommendations expressed in this material are those of the author(s) and therefore funding bodies do not accept any liability in regard thereto.

Appendix A. Supplementary data

Supplementary data to this article can be found online at https://doi.org/10.1016/j.bbih.2019.100027.

References

Barber, A.J., Antonetti, D.A., Gardner, T.W., 2000. The penn state retina Research group: altered expression of retinal occludin and glial fibrillary acidic protein in experimental diabetes. Invest. Ophthalmol. Vis. Sci. 41 (11), 3561–3568.
Bender, C.L., Calfa, G.D., Molina, V.A., 2016. Astrocyte plasticity induced by emotional stress: a new partner in psychiatric physiopathology? Prog. Neuropsychopharm. Biol. Psych. 65, 68–77.
Chandley, M.J., Szebeni, K., Szebeni, A., et al., 2012. Gene expression deficits in pontinelocus coeruleus astrocytes in men with major depressive disorder. J. Psychiatry Neurosci. 38, 276–284.
Chen, Y., Swanson, R.A., 2003. Astrocytes and brain injury. J. Cereb. Blood Flow Metab. 23 (2), 137–149.
Dada, T., 2017. Is glaucoma a neurodegeneration caused by central insulin resistance: diabetes type 4? J. Curr. Glaucoma Pract. 11 (3), 77–79.
Díaz-Coránguez, M., Ramos, C., Antonetti, D.A., 2017. The inner blood-retinal barrier: cellular basis and development. Vis. Res. 139, 123–137.
Ding, F., O'Donnell, J., Thrane, A.S., et al., 2013. α1-Adrenergic receptors mediate coordinated Ca^{2+} signaling of cortical astrocytes in awake, behaving mice. Cell Calcium 54 (6), 387–394.
Du, X., Pang, T.Y., 2015. Is dysregulation of the HPA-Axis a core pathophysiology mediating Co-morbid depression in neurodegenerative diseases? Front. Psychiatry 6, 32.
Enhörning, S., Malan, L., 2019. Copeptin relates to a fatty liver and measures of obesity in a South African population with mixed ethnicities. Endocrine 65, 304–311.
Flammer, J., Konieczka, K., Flammer, A.J., 2013. The primary vascular dysregulation syndrome: implications for eye diseases. Biomed. Cent. EPMAJ 4, 14.
Hansen, G.L., Kofoed, P.K., Munch, I.C., et al., 2012. Retinal angiographic blood flow is reduced in the ocular ischaemic syndrome. Dan. Med. 60, A4716.
Hoebel, S., Malan, L., Botha, J., et al., 2014. Optimizing waist circumference cut-points for the metabolic syndrome and its components in a South African cohort at 3 year follow-up: the SABPA prospective cohort. Endocrine 67 (1), 2014.
Ito, H., Kanno, I., Hatazawa, J., et al., 2003. Changes in human cerebral blood flow and myocardial blood flow during mental stress measured by dual positron emission tomography. Nucl. Med. 17 (5), 381–386.
Jauregui-Huerta, F., Ruvalcaba-Delgadillo, Y., Gonzalez-Castañeda, R., et al., 2010. Responses of glial cells to stress and glucocorticoids. Curr. Immunol. Rev. 6, 195–204.
Kotliar, K., Hauser, C., Ortner, M., et al., 2017. Altered neurovascular coupling as measured by optical imaging: a biomarker for Alzheimer's disease. Sci. Rep. 7, 12906.
Krishnan, V., Nestler, E.J., 2008. The molecular neurobiology of Depression. Nature 455 (7215), 894–902.
Kroenke, K., Spitzer, R.L., 2002. The PHQ-9: a new depression diagnostic and severity measure. Psychiatr. Ann. 32, 1–7.

Kuehn, S., Meißner, W., Grotegut, P., et al., 2018. Intravitreal S100B injection leads to progressive glaucoma like damage in retina and optic nerve. Front. Cell. Neurosci. 12, 312.
Lee, E., Chung, W.S., 2019. Glial control of synapse number in healthy and diseased brain. Front. Cell. Neurosci. 13, 42.
Liew, G., Wang, J.J., 2011. Retinal vascular signs: a window to the heart? Rev. Esp. Cardiol. 64 (6), 515–521.
Lucassen, P.J., Pruessner, J., Sousa, N., et al., 2014. Neuropathology of stress. Acta Neuropathol. 127, 109–135.20.
Malan, L., Hamer, M., Frasure-Smith, N., et al., 2015. Cohort profile: sympathetic activity and ambulatory blood pressure in Africans (SABPA) prospective cohort study. Int. J. Epidemiol. 44 (6), 1814–1822.
Malan, L., Hamer, M., von Känel, R., et al., 2016. Chronic depression symptoms and salivary NOx are associated with retinal vascular dysregulation: the SABPA study. Nitric Oxide–Biol. Chem. 55–56, 10–17.
Malan, N.T., von Känel, R., Smith, W., et al., 2016. A challenged sympathetic system is associated with retinal vascular calibre in a Black male cohort: the SABPA study. In: Lenasi, H. (Ed.), Microcirculation in Health and Disease. InTech. Janeza Trdine, Rijeka, Croatia, ISBN 978-953-51-4801-2, pp. pp135–153.
Malan, L., Schutte, C.E., Alkerwi, A., et al., 2017. Hypothalamic-pituitary-adrenal-axis dysregulation and double product increases potentiate ischemic heart disease risk in a Black male cohort: the SABPA study. Hypertens. Res. 40 (6), 590–597.
Malan, L., Hamer, M., von Känel, R., Lambert, G.W., Delport, R., Steyn, H.S., Malan, N.T., 2017. Chronic defensiveness and neuroendocrine dysregulation reflect a novel cardiac Troponin T cut point: the SABPA study. Psychoneuroendocrinology 85, 20–27.
Mathea, M.R., Newman, E.A., 2006. Glial cells dilate and constrict blood vessels. A mechanism of neurovascular coupling. J. Neurosci. 26, 2862–2870.
Matias, I., Morgado, J., Gomes, F., et al., 2019. Astrocyte heterogeneity: impact to brain aging and disease. Front. Aging Neurosci. 59 (11), 1663–4365.
Paouri, E., Tzara, O., Kartalou, G.I., et al., 2017. Peripheral tumor necrosis factor alpha (TNF-α) modulates amyloid pathology by regulating blood-derived immune cells and glial response in the brain of AD/TNF transgenic mice. J. Neurosci. 37 (20), 5155–5171.
Piepoli, M.F., Hoes, A.W., Agewall, S., et al., 2016. European Guidelines on cardiovascular disease prevention in clinical practice: the Sixth Joint Force of the European Society of Cardiology and other Societies on cardiovascular disease prevention in clinical practice. Eur. Heart J. 5, 1–78.
Sild, M., Ruthazer, E., Booij, L., 2017. Major depressive disorder and anxiety disorders from the glial perspective: etiological mechanisms, intervention and monitoring. Neurosci. Biobehav. Rev. 83, 474–488.
Simard, S., Coppola, G., Rudyk, C.A., et al., 2018. Profiling changes in cortical astroglial cells following chronic stress. Neuropsychopharmacology 43 (9), 1961–1971.
Someya, E., Akagawa, M., Mori, A., et al., 2019. Role of neuron–glia signaling in regulation of retinal vascular tone in rats. Int. J. Mol. Sci. 20 (8), 1952.
Stegenga, B.T., King, M., Grobbee, D.E., et al., 2012. Differential impact of risk factors for women and men on the risk of major depressive disorder. Ann. Epidemiol. 22 (6), 388–396.
Stellwagen, D., Malenka, R.C., 2006. Synaptic scaling mediated by glial TNF-α. Nature 440, 1054–1059.
Torres-Plata, S.G., Nagy, C., Wakid, M., et al., 2016. Glial fibrillary acidic protein is differentially expressed across cortical and subcortical regions in healthy brains and downregulated in the thalamus and caudate nucleus of depressed suicides. Mol. Psychiatry (2), 509–515.
Tynan, R.J., Beynon, S.B., Hinwood, M., et al., 2013. Chronic stress-induced disruption of the astrocyte network is driven by structural atrophy and not loss of astrocytes. Acta Neuropathol. 126 (1), 75–91.
Vujosevic, S., Micera, A., Bini, S., et al., 2015. Aqueous Humor Biomarkers of Müller cell activation in diabetic eyes. Invest. Ophthalmol. Vis. Sci. 56 (6), 3913–3918.
Wentzel, A., Malan, L., Smith, W., et al., 2019. Retinal vasculature reactivity during flicker-light-provocation, cardiac stress and stroke risk in Africans: the SABPA study. Trans. Stroke Res. (10), 485–494.
Wetherell, M.A., Craw, O., Smith, K., 2017. Psychobiological responses to critically evaluated multitasking. Neurobiol. Stress 7, 68–73.
Wheelock, M.D., Harnett, N.G., Wood, K.H., et al., 2016. Prefrontal cortex activity is associated with biobehavioral components of the stress response. Front. Hum. Neurosci. 10, 583.
Wu, H.Q., Wu, H., Shi, L.L., et al., 2017. The association between retinal vasculature changes and stroke: a literature review and Meta-analysis. Int. J. Ophthalmol. 10 (1), 109–114.
Yang, Z., Wang, K.K., 2015. Glial fibrillary acidic protein: from intermediate filament assembly and gliosis to neurobiomarker. Trends Neurosci. 38 (6), 364–374.
Zong, H., Ward, M., Madden, A., et al., 2010. Hyperglycaemia-induced pro-inflammatory responses by retinal Müller glia are regulated by the receptor for advanced glycation end-products (RAGE). Diabetologia 53, 2656–2666.